ME 550: Advances in Biosensors

LAB 2: Synthesize Carbon Dots and Perform Iron Sensing

Sourav Das, Richa Ghosh, Taylor Renze

Abstract

Carbon Dots are a rapidly growing fluorescence detection technique due to their unique structural properties. This ion detection method has been used in many different applications in recent years, such as biological sensing, drug delivery, photodynamic therapy, photocatalysis, and solar cells. Iron is a common ion detected using these sensors because it is one of the essential parameters in the human body and human blood cells. A deficiency of this ion can cause several diseases such as anemia. Detection of Fe^{3+} has been done extensively in the medical industry. One of the rapid iron detections with the fluorescent quenching method is Carbon Dot Sensing (CDS). CDS has shown a promising future in the biosensing industry. Due to its photostability, and non-toxic nature, CDS has proved its capability in the fluorescent biosensing field.

The goal of this lab is to understand the basics of fabrication, and utilization techniques of CDS. In this lab experiment, Carbon dots are synthesized using the bottom-up solution-based approach with glucose solution and mystery solution X. Fabricated carbon dots were then used to detect Fe^{3+} samples (of known concentrations. Two different methods of Fe^{3+} dilution techniques were used to detect different wavelength fluorescence radiation by a microplate reader (Biotek synergy H1). Later, the F_o/F vs concentration of Fe^{3+} calibration plot was generated for each dilution sample. An unknown solution concentration was then determined using one of the F_o/F vs concentration of Fe^{3+} calibration plots. From the plot, the sensitivity and limit of detection of the carbon dots were reported and compared with the data of other carbon dot studies. It was found that the lab-developed biosensor had a high sensitivity and higher detection limit with a stable fluorescence signal. This lab provided the opportunity to understand the fabrication technique, working principle, functionality, types, and characteristics of carbon dots and how its stable fluorescence properties can be utilized in iron sensing in a more detailed fashion. This lab also provides an opportunity to understand how different dilution methods and human expertise in handling the solution affect the final outcome of the experiment.

1. Introduction

The main motivation of this laboratory comes from numerous applications of Carbon Dot Sensing in different types of applications due to its low cost, high sensitivity, large working temperature range, and short response time. During this laboratory, CDS are synthesized and it is applied to sense the concentration of iron ions and the concentration of unknown concentration sample. Carbon dots, CDS, are one of the emerging groups of nanomaterials that have a plethora of potential uses in fluorescence sensing. These bright and stable fluorescence characteristics response and high sensibility and good detection limit are some of the big primary reasons for its wide range of use in biological sensing, drug delivery, photodynamic therapy, photocatalysis, and solar cells.[1] They have distinguishing physiochemical and optical properties such as tunable photoluminescence and quantum yield, as well as unconverted photoluminescence and high light absorption. Along with these features, the high possibility of tuning properties of carbon dots by doping and surface medication renders them a promising candidate for various applications ranging from drug delivery to hydrogen evolution, analyte detection, and more. Carbon dots can be utilized in multicolor microscopic cellular imaging, and anti-counterfeiting applications due to their remarkable fluorescent characteristics, high photostability, and low cytotoxicity [1,2].

The central hypothesis of this lab lies around how carbon dots can be synthesized and how they can be used in iron sensing. Carbon dots can be fabricated by two approaches: Top-down and bottom-up. Top-down methods are those which rely on cutting down macroscale materials to produce carbon nanoparticles. The bottom-up method towards carbon dots is based on solution-based chemical

synthesis followed by polymerization and carbonization of molecular precursors. This bottom-up approach can be subdivided based on the chemical nature of precursors used, namely non-conjugated or conjugated molecules [3]. Iron is one of the most essential metal ions in the human body. The deficiency of iron leads to anemia, and excessive intake of Fe3+ can cause different kinds of diseases, such as cancer, Alzheimer's disease, and Parkinson's syndrome. Therefore, monitoring the Fe3+ level has become important in environmental and biomedical analyses. There are numerous different types of carbon dot-based fluorescence nanoparticle sensors available on the market such as N-dope CDS, N/P co-doped CDS, B/N Co-doped CDS, 2,2′-(ethylene di-oxy) is (ethylamine) - functionalized carbon nanorods (CNRs) and self-assembly-based fluorescent organic nanoparticles. These have been designed to allow the fluorometric detection of the Fe3+ metal ions [4]. Many iron detection procedures can be difficult due to cost and complexity; hence, the detection of iron ions with high sensitivity and selectivity plays a crucial role. Fluorescence analysis using carbon dots has become popular because of its relative ease and accessibility, as well as its high sensitivity, selectivity, high spatial response, and quick response time [5].

Several types of carbon dots have been synthesized, such as quantum dots, carbon nanotubes, polymer diamonds, and nanodiamonds. The structure of carbon dots is a carbon atom with a nitrogen/oxygen base group or polymeric aggregation. [6] The hybridization of carbon dots makes it possible to tune their structure based on particle size, shape, edges, and surface. The structure between discrete atoms and bulk materials contributes to the density of states of CDS. When the particle size reaches below a critical size, the band gap energy increases. This change in bandgap energy is one of the possible ways to tune structure based on numerous applications. However, because of this change in structure and radiative recombination of electrons and holes, different frequencies of fluorescence occur [7]. Infrared to Ultraviolet radiation is emitted from CDS. This can be tuned based on the application. Another advantage of CDS are their photostability and their ability to resist blinking and photobleaching. This makes them different than semiconductor quantum dots and organic dyes [8].

The main objective of this experiment is to understand the bottom-up fabrication technique of carbon dots and how they can be used in iron sensing and concentration detection of unknown samples. Iron ion sensing is a rapidly growing field in the medical industry. Fluorescence-based nanoprobes have become very useful in metal ion sensing due to their high selectivity and recent technological advancements to make them more accessible [9].

In this experiment, we conducted a detailed study on how carbon dots can be fabricated through the bottom-up fabrication technique and followed by getting Fe^{3+} calibration plot and then a quenching reaction of the carbon dots with the unknown sample. We used the ratio of F_0/F vs concentration plots to help to analyze the concentration of the unknown sample. From the result, sensitivity, the linear sensing region, and the limit of detection is estimated.

2. Experimental Method

Carbon Dots Fabrication

The fabrication of the Carbon dots began with mixing 16.56 mL of 200 mM of glucose solution with 1.18 mL of the mystery solution (Solution X) in a scintillation vial. The vial was then closed tightly and placed in the center of a microwave with the rotating plate removed. The mixture was exposed to 750 W for 60-65 seconds. The process was stopped as soon as the transparent mixture started boiling and changed to a light brown color. The container was removed using heat-resistant gloves and cooled to room temperature. 1% (v/v) 1 mM of KCl was added to the mixture. This helped to keep the solution in suspension. The mixture was then filtered through a 0.2 micrometer syringe filter. This removed the possible residual glucose that didn't react.

Fe3+ Calibration Curve

The second step in the process was the preparation of a 3mM solution of FeCl3 in Dl water (10 mM total). Serial dilutions of $FeCl_3$ using a multichannel pipette and 96 well plate was performed.

Dilution example 1:

Columns 2 to 12 (rows A, B, C) were filled with 200 µL of DI water. column 1 (rows A, B, C) were filled with 400 µL of FeCl3 solution. 200 µL of Column 1 (rows A, B, C) were transferred to column 2 (half concentration).

Dilution example 2:

20 µL of DI water was added using a multichannel pipette and a 96-well plate starting in column 2. The volume increased in each progressive column by 20 µL. Once the DI water was added until 180 µL, $FeCl_3$ was added to each column, starting at 180 µL in column 2 and decreasing by 20 µL until the last column. The final volume of each well was 200 µL.

Column 12 wells in both dilutions were used as blank samples with no $FeCl_3$. These wells were filled with 200 µL of DI water. 50 µL of CQD sample was then added to each of the wells and mixed using the pipette.

Microplate Reader

The fluorescence was then measured using the Gen 5 software of Biotek Synergy H1. 405 nm was selected as the excitation wavelength. The emission was scanned from 420 to 600 nm. The data was then saved and used for interpretation.

Unknown Sample Evaluation

The unknown sample was evaluated by adding 200 µL of the unknown sample in triplicate. 50 µL of CQD sample was added and mixed using the pipette. The sample was then read using the same protocols as discussed previously. The data was then saved and used for interpretation.

3. Results

The Stern-Volmer equation, shown below as Equation 1, was used to represent the quenching reaction of the carbon dots. F_0 is the peak fluorescent intensity in the absence of a quencher, also known as the blank in this experiment. F is the peak fluorescent intensity in the presence of the quencher. K_{SV} is the Stern-Volmer constant, which is the slope of the linear calibration plot, and $[Q]$ is the quencher concentration.

$$\frac{F_0}{F} = K_{SV}[Q] + 1 \quad (1)$$

Table 1 below shows the volume of iron added to each of the three columns as mentioned previously in the procedure for dilution example 1. Lines A, B, and C refer to the measured fluorescence of each of the cells.

Column	Fe3+ [uM]	Line A	Line B	Line C
1	**1000**	12464	12393	11884
2	**500**	14281	13964	13782
3	**250**	21427	19368	18414

4	**125**	21941	20857	28767
5	**62.5**	31276	30582	30309
6	**31.25**	39105	37551	37075
7	**15.63**	45336	43578	41553
8	**7.81**	48859	44874	44389
9	**3.91**	49860	47442	46003
10	**1.95**	53835	50700	47832
11	**0.98**	54722	60011	50405
12 (F0)	**0**	65451	60919	67022

Table 1: Iron measurements and Corresponding Fluorescent Intensity for Dilution 1

Table 2 below shows the ratio of fluorescence in a sample with no iron added to each of the other samples in the given column. These ratios were then averaged across columns at each of the iron volume levels, and the standard deviation was found. Figure 1 below shows the linear sensing region found from the data in Table 2. The standard deviations in the linear sensing region were averaged to, then multiplied by 3 to find the Limit of Detection, as shown below in Equation 2.

F0/F Line A	F0/F Line B	F0/F Line C	Avg	STD
5.251	4.916	5.640	5.269	0.362
4.583	4.363	4.863	4.603	0.251
3.055	3.145	3.640	3.280	0.315
2.983	2.921	2.330	2.745	0.361
2.093	1.992	2.211	2.099	0.110
1.674	1.622	1.808	1.701	0.096
1.444	1.398	1.613	1.485	0.113
1.340	1.358	1.510	1.402	0.094
1.313	1.284	1.457	1.351	0.093
1.216	1.202	1.401	1.273	0.111
1.196	1.015	1.330	1.180	0.158

Table 2: Fluorescent Intensity vs. Peak Fluorescent Intensity, Averages, Standard Deviations, Dilution 1

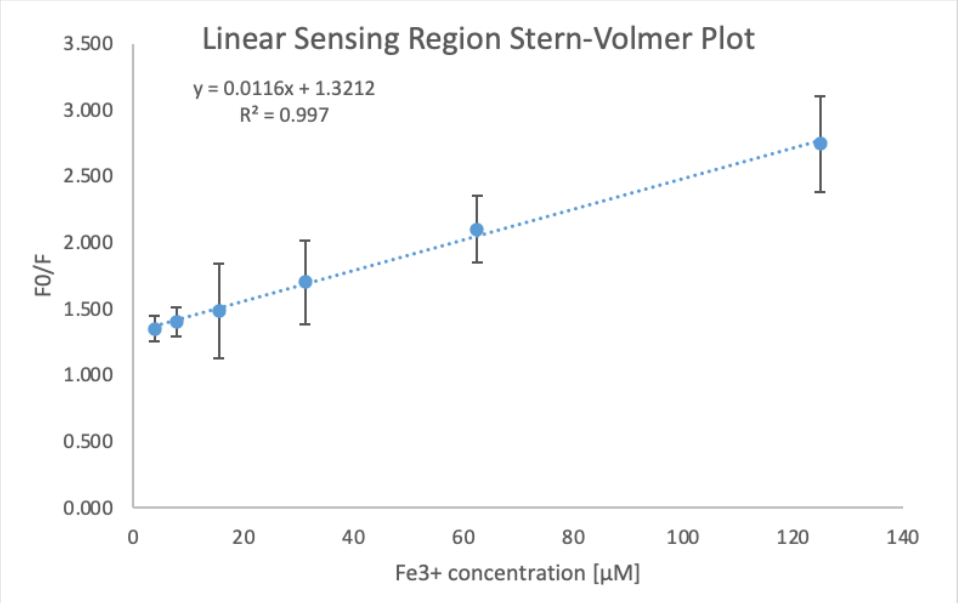

Figure 1: Linear Sensing Region of Dilution 1

$$Limit\ of\ Detection = 3\sigma \quad (2)$$

The average standard deviation for dilution 1 was found to be 0.144. The limit of detection was then found to be 0.4327. Using this data, the calculated unknown sample was found to have a concentration of 167.356 µM iron. The slope of the response vs concentration curve is 0.0116 which can be considered as the sensitivity of fabricated CDs.

Table 3 below shows the volume of iron added to each of the three columns as mentioned previously in the procedure for dilution example 2. Lines A, B, and C refer to the measured fluorescence of each of the cells.

Column	Fe3+ [uM]	Line A	Line B	Line C
1	**1000**	12678	11901	11806
2	**900**	7760	7511	7310
3	**800**	8427	7863	7497
4	**700**	13714	13158	12965
5	**600**	8027	7769	7280
6	**600**	7336	6155	5713
7	**400.00**	15425	15889	16349
8	**300.00**	16787	20455	20922
9	**200.00**	43913	51258	49951
10	**100.00**	22003	31294	30269
11	**500.00**	12679	14854	14351
12 (F0)	**0**	35291	46489	44571

Table 3: Iron measurements and Corresponding Fluorescent Intensity for Dilution 2

Table 4 below shows the ratio of fluorescence in a sample with no iron added to each of the other samples in the given column. These ratios were then averaged across columns at each of the iron volume levels, and the standard deviation was found. Figure 2 below shows the linear sensing region found from the data in Table 4. The standard deviations in the linear sensing region were averaged to, then multiplied by 3 to find the Limit of Detection, as shown in Equation 2.

F0/F Line A	F0/F Line B	F0/F Line C	Avg	STD
2.784	3.906	3.775	3.488	0.614
4.548	6.189	6.097	5.612	0.922
4.188	5.912	5.945	5.348	1.005
2.573	3.533	3.438	3.181	0.529
4.397	5.984	6.122	5.501	0.959
4.811	7.553	7.802	6.722	1.660
2.288	2.926	2.726	2.647	0.326
2.102	2.273	2.130	2.168	0.091
0.804	0.907	0.892	0.868	0.056
1.604	1.486	1.472	1.521	0.072
2.783	3.130	3.106	3.006	0.193

Table 4: Fluorescent Intensity vs. Peak Fluorescent Intensity, Averages, Standard Deviations, Dilution 2

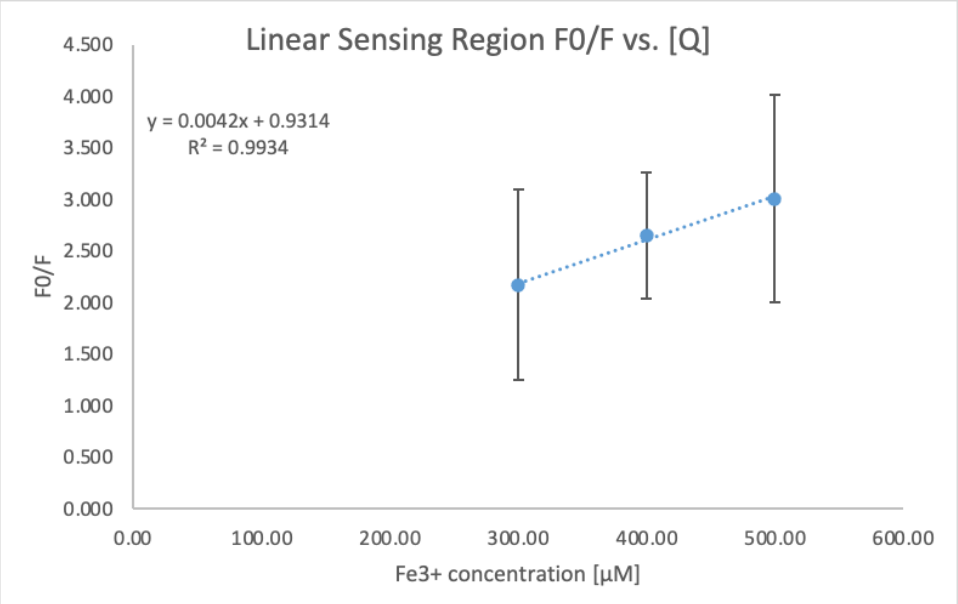

Figure 2: Linear Sensing Region of Dilution 2

The average standard deviation for dilution 1 was found to be 0.204. The limit of detection was then found to be 0.611. Using this data, the calculated unknown sample was found to have a concentration of 463.98 µM iron. The slope of response vs concentration curve is 0.0042 which can be considered as sensitivity of fabricated CDs.

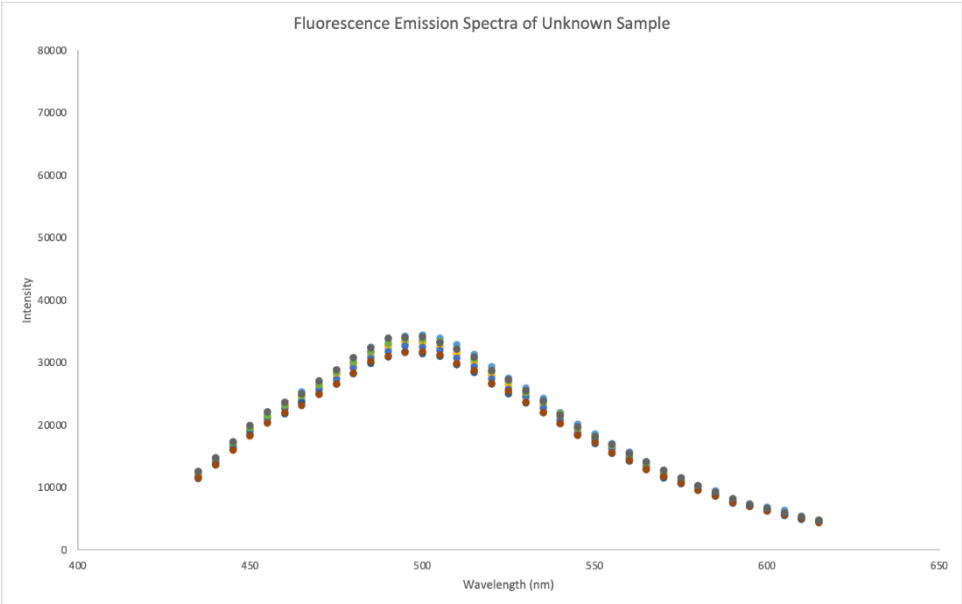

Figure 3: Fluorescence Emission Spectra of Unkown Sample

4. Discussion

In this experiment, several design criteria such as sensitivity, detection limit, response time etc. has been studied with varying concentration of Fe^{+3}ions for quenching purpose of CND/CQDs/CQDsHG. Stern-Volmer equation has been one such calibration curve that has been used.

In the Lab, two different methods of diluting sample Fe^{3+} and QDs are used. For this, two different calibration curves have been plotted.

K_{sv} of the Stern-Volmer equation is an important parameter for determining the type of fluorescence quenching. For dynamic quenching process, K_{sv} decreases as the temperature increases, while in the while it is opposite for static quenching process. The mechanism of dynamic quenching is that the fluorescence intensity gets reduced by the collision of quencher and fluorophore. Hence, the loss of the excited state energy caused by the collision makes the excited state return to the ground state. Increasing the temperature causes the diffusivity coefficient to increase, which leads to K_{sv} to increases with the increasing of temperature. Static quenching on the other hand is a process in which non-fluorescence or weak fluorescence compounds are formed as a result of reaction between the quencher and fluorophore which will lead to reduction in the fluorescence intensity. The K_{sv} static quenching decreases with the increasing of temperature, because of the reduction in the stability of complex. [11] Therefore, exploring the fluorescence quenching effect of Fe^{+3} ions in the NPs solution at different temperatures should be done. [11]

Excitation wavelength 405 nm for all the experiments conducted as cited in Table 5.

Refer-ence	**Method**	**Sensitivity**	**Detection Limit 3σ (µM)**	**Sensing Range (µM)**	R^2	**Calibration curve**	**Response time**
[10]	CDs for iron sensing	-0.00358	3.8	8-80	0.9936	$\frac{F}{F_o} = -0.00358x + 1.00875$	--
[9]	Fluorescence to monitor iron	0.013	0.76	2.50–150	0.99884	$\frac{F_o}{F} = 0.013x + 1.01$	5.0 mins
[11]	CQDs for iron sensing	1.34×10^5	0.172	1-50	0.993	$\frac{F_o}{F} = 0.4899x + 1$	--
[12]	CNDs for iron sensing	-0.006	0.180	0-100	0.9932	$\frac{F}{F_o} = -0.006x - 0.003$	--
[13]	CQDsHG for iron sensing	-0.00254	0.24	0-150	0.993	$\frac{F}{F_o} = -0.00254x + 0.992$	--
[14]	Electrochemical iron sensors based on reduced graphene oxide/gold nanoparticles modified electrode	0.003	0.0035	30 nM-3 µM	0.9946	$I_p = 0.003x + 0.0063$; I_p is the peak current which is linear with the concentration of Fe(III) ions.	--
This work: (1) represents Dilu	CDs for iron sensing	1. 0.0116 2. 0.0042	1. 0.4327 2. 0.611	1. 0-140 2. 300-500	1. 0.997 2. 0.9934	1. $\frac{F_o}{F} = 0.0116x + 0.3212$ 2. $\frac{F_o}{F} = 0.0042x - 0.0686$	--

tion 1 (2) repr esen ts Dilu tion 2							--

Table5. Comparative Literature Survey of Carbon Nanoprobles for detection of Fe^{+3} Metal ion sensing

From Table 5. we can see that the sensitivity from Dilution 1 is more sensitive than that of Thursday's experiment. Also, juxtaposing with the Literature survey conveys that both the readings obtained from Dilution 1 & 2 falls in the range. The linear fit to the calibration curve R^2 is also falls within the range obtained from the literature survey.

Table 5. also highlights the range of sensitivities, detection limit, sensing range, calibration curves as obtained by different techniques (CD/QDs), electrochemical iron sensors in different conditions, Ph ranges, and concentration range of Fe^{+3}.

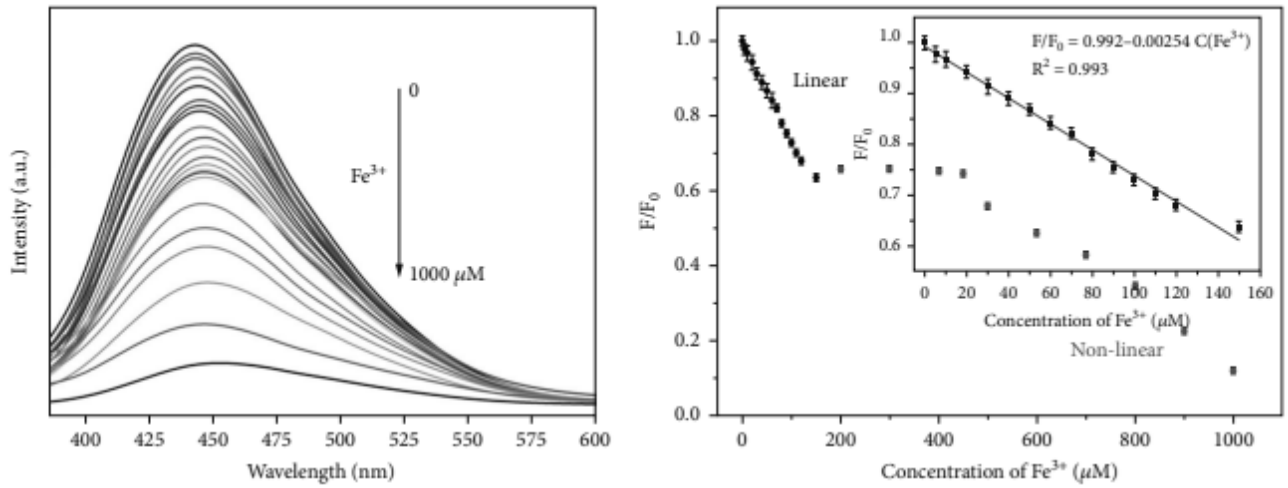

Figure 4: (a) Fluorescence emission spectra of the CQDsHG upon exposure to various concentrations of Fe3+ solutions (from top to bottom: 0, 5, 10, 20, 30, 40, 50, 60, 70, 80, 90, 100, 110, 120, and 150 μM) under excitation at 370 nm and (b) the calibration curves and linear equation for the fluorescence quenching ratio and concentration of Fe3+. [13]

From paper [13] Carbon quantum dots/hydrogel nanocomposites materials (CQDsHG) served as good fluorescence detection of Fe^{+3} ions. The CQDs were prepared using a microwave-assisted method for 15 mins like what has been conducted in the laboratory. Then the CQDs were loaded into the hydrogel using the sol-gel method. The sensitivity of fabricated CDs found for two different dilution techniques is 0.0042 and 0.0116. The detection limit was found to be 0.24 μM in the range of 0–150 μM whereas for our experiments, the detection limit was found to be 0.4327 μM within the range 0-140 μM and 0.611 μM within the range 300-500 μM. The R^2 fit for paper [13] and our work are 0.993 and 0.997, 0.9934. Compared to literature [13] our detection limit is on the higher range. A lower detection limit represents easier detection of Fe^{+3} even at lower concentrations. The lower detection limit can be estimated due to human error while preparing the sample and maybe if the carbon dots are loaded in the hydrogel, might increase the sensitivity as has been identified in [13].

The variation in the sensitivity between the two dilutions from Tuesday and Thursday's lab results can be perceived due to the insufficient amount of data collected and it will do good if repeated calibration tests were conducted using the same method which might result in less standard deviation. Also, the samples were prepared by a comparative novice student who is not accustomed to pipettes, changing of the tips, and lacking the skills required for dilution of the sample as was frequently required. Hence human error while conducting the experiment has most likely occurred leading to the variation in the results. All of these can be circumscribed by conducting more experiments and inculcating the required skills before getting the data. Moreover, for future experiments, combination of hydrogel along with the produced carbon dots in the mystery solution can be experimented with to see whether improvements can be made. Another viable step that can be taken for future labs is exploring the fluorescence quenching effect of ions in the NPs solution at different temperatures.

5. Conclusion

Current research in the field of carbon dot synthesis and detection is particularly important for many applications. There has been a small amount of research related to the fluorescent detection of iron ions using carbon dots. Detecting the amount of iron in humans is important because outside of specific ranges, several different severe diseases and illnesses can occur. By using microwaves to synthesize carbon dots in this laboratory, the group successfully analyzed iron concentrations using accessible materials which produced results with high sensitivity and selectivity. The results were found to be comparable to those obtained by other groups and in other published works, as referenced in Table 5.

Dilution 1 resulted in a limit of detection of 0.4327 and a sensitivity of 0.0116. Using this data, the calculated unknown sample had a concentration of 167.356 μM iron. Dilution 2 resulted in a limit of detection of 0.611, and a sensitivity of 0.0042. Using this data, the calculated unknown sample was found to have a concentration of 463.98 μM iron.

This laboratory helped establish one of the many methods of synthesizing carbon dots and what to avoid or improve in future experiments. The results from dilution 2 were subject to human error and should not be considered accurate. Futuristically, the precision of the lab equipment should be more closely considered. It should also be noted that the microwaving process is extremely specific, and any slight deviation may ruin the carbon dots.

Another future consideration could be to use hydrogel to create the matrices for carbon dot sensors. According to a study done on "Carbon Quantum Dots-Based Fluorescent Hydrogel Hybrid Platform for Sensitive Detection of Iron Ions," many carbon dot applications require solid matrices for effective ion detection [13]. Because of hydrogel applications in class discussions, it would be interesting to follow the procedure of this study to better understand how hydrogels and carbon dots interact with one another. It would also be interesting to compare the results of iron detection using a hydrogel as compared to an aqueous solution and exploring the effect of varying the temperature on K_{sv} and hence determining the quenching mechanism.

7. References

1. Samahe Sadjadi, "Chapter 4 - The utility of carbon dots for photocatalysis", Emerging Carbon Materials for Catalysis, Elsevier, 2021, Pages 123-160, ISBN 9780128175613, https://doi.org/10.1016/B978-0-12-817561-3.00004-4
2. Chen Li, Xiaoyan Sun, Yuan Li, Hailu Liu, Bibo Long, Dong Xie, Junjia Chen, and Ke Wang , "Rapid and Green Fabrication of Carbon Dots for Cellular Imaging and Anti-Counterfeiting", Applications ACS Omega 2021 6 (4), 3232-3237, DOI: 10.1021/acsomega.0c05682

3. Döring, A., Ushakova, E. & Rogach, A.L. Chiral carbon dots: synthesis, optical properties, and emerging applications. *Light Sci Appl* **11**, 75 (2022). https://doi.org/10.1038/s41377-022-00764-1
4. Chumki Dalal, Anjali Kumari Garg, Manas Mathur, and Sumit Kumar Sonkar, ACS Applied Nano Materials 2022 5 (9), 12699-12710 DOI: 10.1021/acsanm.2c02544
5. Khairy GM, Amin AS, Moalla SMN, Medhat A, Hassan N. Fluorescence determination of Fe(iii) in drinking water using a new fluorescence chemosensor. RSC Adv. 2022 Sep 28;12(42):27679-27686. doi: 10.1039/d2ra05144c. PMID: 36276051; PMCID: PMC9516559.
6. S. Zhu et al., The photoluminescence mechanism in carbon dots (graphene quantum dots, carbon nanodots, and polymer dots): current state and future perspective, Nano Res., 2015, 8 , 355 —381
7. Molaei, Mohammad Jafar, "Principles, mechanisms, and application of carbon quantum dots in sensors: a review", Anal. Methods, 2020,12, 1266-1287, https://doi.org/10.1039/C9AY02696G
8. F. Yuan et al., Shining carbon dots: synthesis and biomedical and optoelectronic applications, Nano Today, 2016, 11 , 565 —586
9. Yeung, M. C. L.; Yam, V. W. W. Luminescent cation sensors: from host−guest chemistry, supramolecular chemistry to reactionbased mechanisms. Chem. Soc. Rev. 2015, 44, 4192−4202
10. Chen Yanqiu, et al. "Fe3+-Sensitive Carbon Dots for Detection of Fe3+ in Aqueous Solution and Intracellular Imaging of Fe3+ Inside Fungal Cells." Frontiers in Chemistry, vol. 7, 2020, ISSN=2296-2646, doi. 10.3389/fchem.2019.00911
11. Z. Nan, C. Hao, X. Zhang, H. Liu, R. Sun, Carbon quantum dots (CQDs) modified ZnO/CdS nanoparticles based fluorescence sensor for highly selective and sensitive detection of Fe(III), Spectrochimica Acta Part A: Molecular and Biomolecular Spectroscopy (2019), doi: https:// doi.org/10.1016/j.saa.2019.117717.
12. Zhang, Xianfeng & Lu, Jingbo & Zhou, Xiaoli & Guo, Chunyan & Wang, Chuanhu. (2017). Rapid microwave synthesis of N-doped carbon nanodots with high fluorescence brightness for cell imaging and sensitive detection of iron (III). Optical Materials. 64. 1-8. 10.1016/j.optmat.2016.11.026.
13. Wu, Shunwei, et al. "Carbon Quantum Dots-Based Fluorescent Hydrogel Hybrid Platform for Sensitive Detection of Iron Ions." *Journal of Chemistry*, vol. 2022, 2022, pp. 1–14., https://doi.org/10.1155/2022/3737646.
14. Yun Zhu, Dawei Pan, Xueping Hu, Haitao Han, Mingyue Lin, Chenchen Wang, An electrochemical sensor based on reduced graphene oxide/gold nanoparticles modified electrode for determination of iron in coastal waters, Sensors and Actuators B: Chemical, Volume 243, 2017, Pages 1-7, ISSN 0925-4005, https://doi.org/10.1016/j.snb.2016.11.108.